15–20 × 10^6 MSCs injected. After the surgery, the graved rats were treated with 0.05 mg/kg buprenorphine (Torpan, Maillefer, Switzerland) as an analgesic, and kept in a temperature-controlled room with a 12-h alternating light–dark cycle until E21. Water and food were provided ad libitum throughout the experiment.

Tissue extraction

On E21, the pregnant rats were sedated and killed via cesarean section under anesthesia with the intraperitoneal injection of pentobarbital. In each case, the fetus was opened using a midline incision, and the presence of a left-sided diaphragmatic hernia was confirmed. The lung tissue was removed, with the left lung used for the analysis. All lungs were transversely dissected in a similar manner with symmetrical slices, and the medial portion of the lungs was fixed in 10 % formalin solution for 24 h and embedded in paraffin for the morphological analysis.

Histology and morphometric analysis

Formalin-fixed, paraffin-embedded, 4-μm-thick lung sections were stained with hematoxylin–eosin (HE). At least six photographs of randomly selected microscopic fields were analyzed per animal. The pulmonary alveolar wall thickness was assessed by measuring the thicknesses of five of the thinnest alveolar wall sections per field in ~50 fields per group, using a previously described method [16–18]. The quantitative lung morphometry assessment was performed using the NIH ImageJ software program at 200× magnification.

Immunohistochemistry and pulmonary artery morphometry

Immunohistochemistry was performed using formalin-fixed, paraffin-embedded lung tissues. The primary antibodies included a mouse anti-proliferating cell nuclear antigen antibody (PCNA, Dako, 1:100), rabbit polyclonal antibody against surfactant protein-C (SP-C) (Santa Cruz, 1:200), monoclonal antibody to α smooth muscle actin (αSMA) (Sigma, 1:5000), and rabbit polyclonal antibody to green fluorescent protein (GFP) (Abcam, 1:500).

The number of PCNA-positive cells was manually counted using a grid with the assistance of the ImageJ software program and expressed as the percentage of positive staining cell over the total cell number/field. Cells with strong brown nuclear staining were considered to be PCNA-positive. Brown cytoplasmic cell staining was considered to indicate SP-C-positive cells. The number of SP-C-positive cells over the total cell number/field was also manually counted. Both the analyses of PCNA and SP-C were limited to the air exchanging parenchyma only, excluding large airways and vessels.

The thicknesses of medial walls of arteries stained with α-SMA antibodies were calculated using a formula previously described in the literature [19]. Only fully muscularized vessels with the external diameter less than 100 μm were included in the analysis [20].

Statistical analysis

The data were analyzed statistically using the IBM SPSS Statistic 20 software package. A one-way ANOVA and the Mann–Whitney U test were used in accordance with the data distribution. The Shapiro–Wilk test was used to confirm the normality of the data. A p value of <0.05 was considered to be statistically significant.

Results

Morphology and cell characteristics

The population of cells derived from the adult lung eGFP transgenic rats was expanded in the culture dish; the cells exhibited a spindle shape and fibroblast-like morphology (Fig. 1a). In addition, the cells had the ability to adhere to the tissue culture dish, with proliferation and growth into small colonies. The number of colonies of various sizes increased, demonstrating proliferation and expansion throughout the whole plastic surface until confluence (Fig. 1b). Passage 3 of the MSC culture displayed a monomorphic appearance with spindle cells in the culture. The cultured cells differentiated into three lineages, including osteoblasts, adipocytes, and chondroblasts in the in vitro study (data not shown).

Alveolar parenchymal morphology

The lung morphology of the fetuses in the CDH group was significantly different to that observed in the normal lungs based on an analysis of the alveolar wall thickness and alveolar air space area. The alveolar walls in the CDH group were thicker than those noted in the control group (10.84 μm, range 9.85–12.08 vs. 7.81 μm, range 7.18–8.58 μm, respectively; $p = 0.000$) (Fig. 2a; Table 1). Meanwhile, the alveolar air space area per field in the CDH group was smaller than that observed in the control group (0.028 mm^2, range 0.026–0.032 vs. 0.056 mm^2, range 0.053–0.061 mm^2, respectively; $p = 0.000$) (Fig. 2a; Table 1). MSC transplantation significantly decreased the alveolar wall thickness (8.77 μm, range 7.91–9.61 vs. 10.84 μm, range 9.85–12.08 μm,

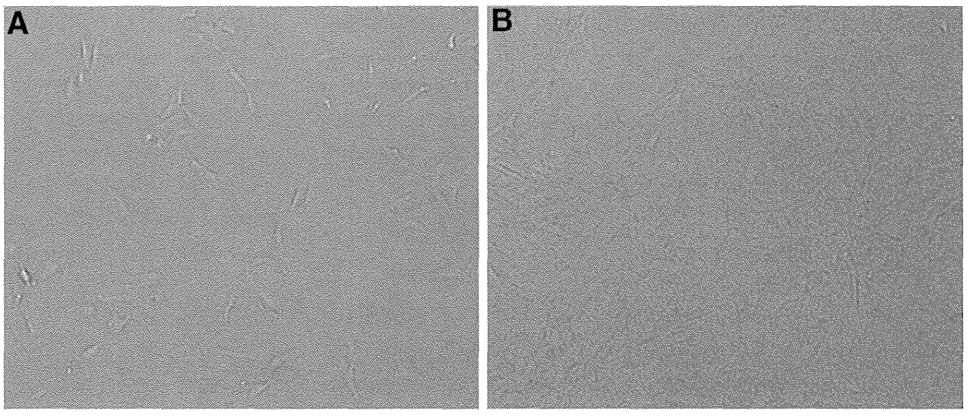

Fig. 1 Morphology of the mesenchymal stem cells in culture. **a** Appearance of the mesenchymal stem cell culture of passage 3 on day 3. **b** Passage 3 of the MSC culture on day 7 (magnification: **a**, **b** ×100)

respectively; $p = 0.000$) and the increased alveolar air space area compared to that observed in the CDH group (0.041 mm^2, range 0.038–0.046 mm^2/field vs. 0.028 mm^2, range 0.026–0.032 mm^2/field, respectively; $p = 0.000$). The alveolar wall thicknesses in the MSC-treated CDH and control groups were 8.77 μm (range 7.91–9.61 μm) and 7.81 μm (range 7.18–8.58 μm; $p = 0.000$), respectively, while the alveolar air space area was 0.041 mm^2 (range 0.038–0.046 mm^2)/field and 0.056 mm^2 (0.053–0.061 mm^2/field; $p = 0.000$), respectively. These findings were consistent with the microscopic appearance, in which the lungs in the control group displayed well-developed saccules, thin alveolar walls and well-expanded air space areas. In contrast, the CDH lungs exhibited thickened alveolar walls with compacted tissue and undeveloped saccules.

Cell proliferation

Anti-proliferating cell nuclear antigen was used as a marker of cell proliferation. In the analysis, the immunoreactivity of PCNA was confined to the nucleus, with positive nuclei expressing strong brown staining. PCNA-positive cells were more numerous in the lung parenchyma of the control group than in that observed in the CDH group (Fig. 2b). In all groups, within the air exchanging parenchyma, PCNA-positive cells were mostly found in the interstitial areas of the lungs. The proportion of proliferating cells/field in the CDH group was significantly decreased compared to that observed in the control group, at 2.18 % ± 1.224 vs. 10.22 % ± 4.460/field, respectively ($p = 0.000$) (Fig. 3a). In addition, the proportion of PCNA-positive cells was significantly increased in the MSC-treated CDH group, at 8.32 % ± 4.018/field compared with the 2.18 % ± 1.224/field observed in the CDH group ($p = 0.000$). The proportion of PCNA-positive cells had no significant differences between the MSC-treated CDH group and the control group [8.32 % ± 4.018 vs. 10.22 % ± 4.460/field, respectively ($p = 0.140$)].

Lung maturation

Surfactant protein-C is a specific marker for alveolar type II cells. SP-C-positive cells were clearly visualized as brown cytoplasmically stained cells in the epithelial lining of the alveolar wall. In the CDH group, the SP-C expression was very faint and almost not detected (Fig. 2c). In addition, the proportion of SP-C-positive cells per field was significantly decreased in the CDH group compared with that observed in the control group, at 0.57 % ± 0.791 vs. 11.47 % ± 2.762/field, respectively ($p = 0.000$) (Fig. 3b). In contrast, MSC transplantation significantly enhanced the SP-C expression in the nitrofen-induced left-CDH fetuses, with the number of SP-C-positive cells being higher (10.16 % ± 2.912/field; $p = 0.000$) than that observed in the CDH group. In contrast, there were no significant differences in the SP-C expression between the control and MSC-treated CDH groups.

Pulmonary artery morphometry

The muscular layer of the arteries in the CDH group was thicker than that observed in the control group (Fig. 2d). In addition, the medial thickness index of the pulmonary arteries was significantly higher in the CDH group (0.25 ± 0.096) than in the control group (0.22 ± 0.070; $p = 0.011$) (Fig. 3c), while the medial thickness index of the arteries in the MSC-treated CDH group was significantly lower than that observed in the CDH group (0.22 ± 0.08 vs. 0.25 ± 0.096, respectively; $p = 0.024$). There were no significant differences in the medial thickness index between the control and the MSC-treated CDH groups ($p = 0.933$). The degree of medial hypertrophy relative to the external diameter is represented by the medial thickness index.

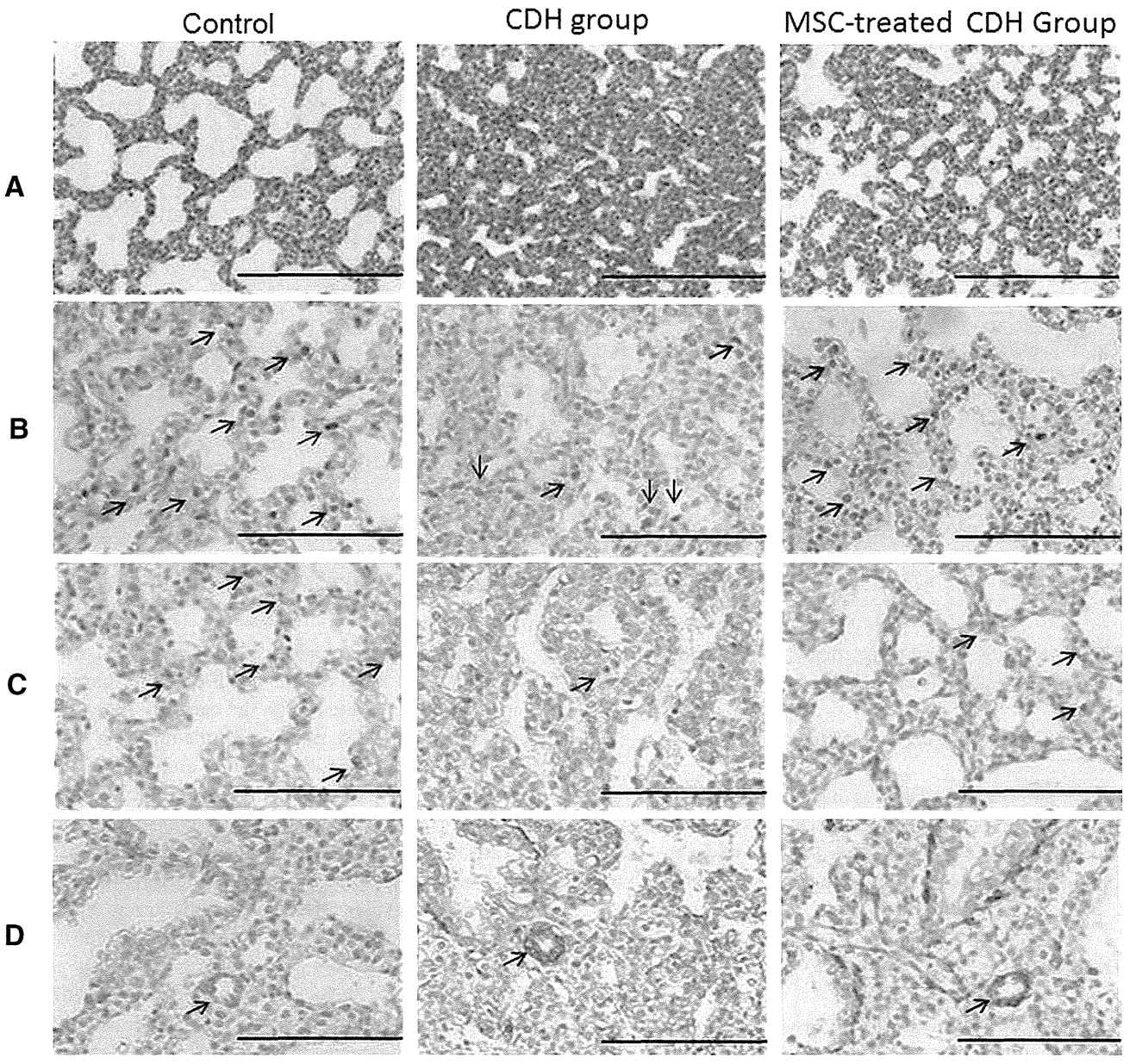

Fig. 2 Morphological analysis of HE staining and immunohistochemistry. Tissues stained with **a** Hematoxylin–eosin (HE). **b** Immunohistochemical staining for PCNA. The *arrow* indicates PCNA-positive cells. **c** Immunohistochemical staining for SP-C. The *arrow* indicates SP-C-positive cells. **d** Immunohistochemical staining for alpha smooth muscle actin. The *arrow* indicates the medial thickness in the pulmonary arteries (magnification: **a** ×200, **b–d** ×400). *Scale bars* **a** 200 μm, **b–d** 100 μm

Table 1 Morphometrical analysis of the lungs

Morphometrical analysis	Control	CDH	MSC-treated CDH
Alveolar wall thickness (μm)	7.81 μm (7.18–8.58)	10.84 μm (9.85–12.08)*	8.77 μm (7.91–9.61)*, #
Alveolar air space area (mm^2/field)	0.056 mm^2 (0.053–0.061)	0.028 mm^2 (0.026–0.032)*	0.041 mm^2 (0.038–0.046)*, #

The data are presented as the median (25th–75th percentile), * $p < 0.001$, compared to the control group, # $p < 0.001$, compared to the CDH group

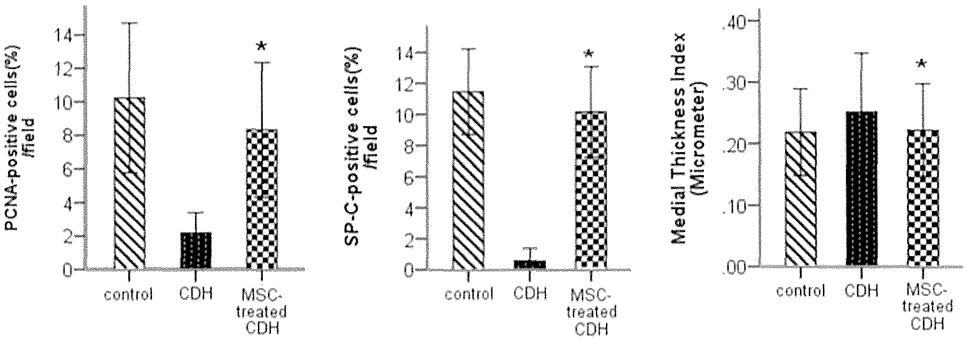

Fig. 3 Quantitative analysis of individual markers. The quantitative expression of proliferating cell nuclear antigen (**a**), surfactant protein-C (**b**), and the medial thickness index (α-SMA) (**c**) among the three groups. The data are presented as mean ± SD. $^{*}p < 0.05$ compared with the CDH group

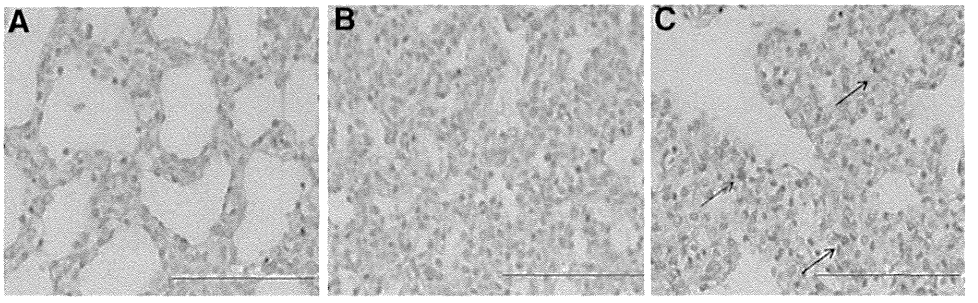

Fig. 4 Engraftment of the MSCs in the lung tissue. **a** Control group, **b** CDH group, **c** MSC-treated CDH group. In the MSC-treated CDH group, there was a positive GFP cell expression in the interstitial lungs (magnification **a**–**c** ×400). *Scale bars* **a**–**c** 100 μm

Therefore, MSC therapy significantly decreased the degree of muscularization of the pulmonary arteries.

Mesenchymal stem cell engraftment

In the MSC-treated CDH group, the expression of green fluorescent protein (GFP)-positive cells was observed in the lung parenchyma (Fig. 4c), particularly in the interstitial areas of the lungs, presenting as brown-stained cells.

Discussion

Severely hypoplastic lung diseases and associated persistent pulmonary hypertension remain as serious causes of morbidity and mortality in CDH patients, despite advances in postnatal interventions, such as the advent of inhaled nitric oxide (iNO), extracorporeal membrane oxygenation (ECMO), high-frequency oscillatory ventilation (HFO) and gentle ventilation [1, 2]. The TOTAL trial requires additional time to investigate the efficacy of these treatments in terms of improving the morbidity of moderate and mortality of severe CDH [7, 8]. At present, half of fetuses cannot be salvaged with FETO [7]. One reason for this high mortality rate is that FETO simply does not trigger adequate lung development. Several reports have attempted to demonstrate the efficacy of peptides, hormones, and alternatives in experimental models of CDH, although the results have shown limited effects with respect to lung morphogenesis [3–6].

Recent advances in stem cell biology appear to be very promising and attractive, as such cells are unspecialized and/or undifferentiated, with the capacity for self-renewal and the power to give rise to multiple different specialized cell types [7, 21]. The activation of endogenous lung stem cells may increase the number and size of bronchopulmonary segments, whereas exogenous stem cells contribute to lung development [10]. Such cells may have a direct effect due to the integration, differentiation, and/or activation of resident stem cells via paracrine mechanisms [10]. The paracrine immunomodulation of stem cells and their protective effects against parenchymatous and vascular lung injury have previously been demonstrated in several models of lung injury [12, 19]. In particular, MSCs are ideal because they can modulate damage due to their potent immunosuppressive effects [10, 12, 22]. In addition, several experimental studies have shown that treatment with MSCs can reverse lung parenchymal fibrosis, pulmonary injury, and pulmonary hypertension [10, 12, 14]. However, it is important to note that MSCs represent a 'heterogeneous' population, expressing different levels of a panel of characteristic cell surface markers. MSCs are further defined by their properties of cell attachment, self-renewal, clonogenicity and the ability to differentiate towards multiple lineages [23, 24]. In the present study, cultured cells derived from the minced lungs of eGFP rats were found to have the capacity to adhere to the plastic culture surface, with a spindle-shape morphology, and both proliferative and clonogenic abilities. The cells also demonstrated the capability to

differentiate into osteoblasts, adipocytes, and chondroblasts in vitro; these characteristics reflect mesenchymal stem cell properties.

Cell-based therapy approaches to treating lung diseases have focused on using non-resident stem cells, particularly bone marrow MSCs (BMSCs); however, given the engraftment capacity of BMSCs after transplantation and the possible lung phenotypes after transplantation, there are inconsistent results as to whether BMSCs truly engraft and differentiate into lung phenotypes [14, 25]. Recent studies have also demonstrated the presence of "mesenchymal-like" progenitor cells in the lungs with a multipotent regenerative and high proliferative capacity, with the expectation that lung-derived MSCs will more easily respond to the local lung milieu, thus promoting engraftment and regeneration [12, 25]. Although it remains controversial, MSCs derived from various organs may exhibit tissue-specific differences with various epigenetic features.

Mesenchymal stem cells have the ability to transfer and engraft from maternal to the fetal body. Chen et al. [26] showed that human MSCs from maternal origin have the ability to traffic through the placenta to the fetal tissue in the pregnant rat model. Placenta expresses vascular endothelial growth factor A (VEGF-A) and it may be secreted into the fetal blood. The level of VEGF-A is higher in the fetal circulation than the maternal circulation, showing a concentration gradient from maternal to fetal circulation. High concentration of VEGF-A in the fetal blood may play a role in the mobilization of maternal circulating stem cells.

Nitrofen-induced CDH model rats demonstrate diaphragmatic defects, hypoplastic lungs and pulmonary vascular anomalies, in which the diaphragmatic defect is produced during the course of lung development [3–6]. Lung morphogenesis specifically requires an interaction between the epithelia and mesenchyme, identified as the epithelial–mesenchymal interaction [27]. The extent of induction is dependent on the amount of mesenchyme, and the proximal lung bud epithelium requires continuous stimulation from the distal mesenchyme. In the present study, the fetal lung hypoplasia appeared to have improved, as indicated by the enlargement of air space area and a decrease in the alveolar wall thickness. MSC transplantation may, therefore, enhance cell proliferation, as indicated by increases in the number of PCNA-positive cells and the SP-C expression. MSC transplantation may also decrease the degree of muscularization of the pulmonary arteries, as evidenced by the decrease in the medial thickness index. In addition, the expression of GFP-positive cells was observed in the mesenchyme of the lungs, and the proportion of GFP-positive cells/field seems lower than that of PCNA-positive cells/field in the MSC-treated CDH group. Based on these results, we hypothesize that the MSCs transplanted via the uterus vein engrafted into the fetal lung parenchyma, where they promoted the epithelial–mesenchymal interaction, thus ameliorating lung hypoplasia. However, there are several limitations associated with this study, as we did not perform a molecular biological study so as to identify the signaling pathways and/or elucidate the molecular roles of these cells in proliferation and differentiation. We are preparing to perform such studies in the near future.

Mesenchymal stem cells display a broad spectrum of potential effects, including immunomodulatory, antifibrotic, and trophic actions, on resident tissue progenitor cells, features that suggest the critical role of these cells in tissue homeostasis, and serve as the basis for their application in cellular therapy [12, 21, 24]. The therapeutic effects of MSCs in lung disease not only include their derived capacity to migrate to the sites of injured tissue, but also their ability to interact with injured host cells and secrete paracrine soluble factors that can alter the response of the endothelium and epithelium to injury via the release of growth factors [12–14, 28]. Indeed, the paracrine immunomodulation of MSCs and their protective effect against parenchymatous and vascular lung injury have previously been reported in several models of lung injury [10, 14, 15]. The main paracrine factors secreted by MSCs are growth factors and their corresponding receptors, some of which include VEGF, FGF, TGF, HGF, angiopoietin, etc. In addition these cells have the capacity to secrete cytokines and chemotactic factors, as well as regulatory peptides and stem cell-specific active factors; these soluble paracrine factors have various effects on the respiratory epithelium, endothelial cells, smooth muscle cells and fibroblasts in the lungs [29, 30]. Although, some studies have demonstrated the efficacy of treatment with amniotic-derived MSCs in nitrofen-induced CDH animal models, the mechanisms underlying both the development of lung damage and repair in the setting of CDH remain to be fully elucidated [31, 32].

Conclusion

The present results demonstrate that MSCs derived from adult rat lungs have the capacity of engraftment into the fetal lung parenchyma. Therefore, MSC transplantation may promote cell proliferation and differentiation in nitrofen-induced CDH model rats, thus suggesting that MSC therapy may have therapeutic potential to ameliorate pulmonary hypoplasia and pulmonary hypertension.

Acknowledgments The authors wish to thank Mr. Brian Quinn for supporting the manuscript. This work was supported in part by a Grant-in-Aid for Scientific Research from the Japanese Society for the Promotion of Science.

Conflict of interest The authors do not have any conflicts of interest related to this paper.

References

1. Masumoto K, Teshiba R, Esumi G, Nagata K, Takahata Y, Hikino S, Hara T, Hojo S, Tsukimori K, Wake N, Kinukawa N, Taguchi T (2009) Improvement in the outcome of patients with antenatally diagnosed congenital diaphragmatic hernia using gentle ventilation and circulatory stabilization. Pediatr Surg Int 25:487–492
2. Nagata K, Usui N, Kanamori Y, Takahashi S, Hayakawa M, Okuyama H, Inamura N, Fujino Y, Taguchi T (2013) The current profile and outcome of congenital diaphragmatic hernia: a nationwide survey in Japan. J Pediatr Surg 48:738–744
3. Takayasu H, Nakazawa N, Montedonico S, Sugimoto K, Sato H, Puri P (2007) Impaired alveolar epithelial cell differentiation in the hypoplastic lung in nitrofen-induced congenital diaphragmatic hernia. Pediatr Surg Int 23:405–410
4. Esumi G, Masumoto K, Teshiba R, Nagata K, Kinoshita Y, Yamaza H, Nonaka K, Taguchi T (2011) Effect of insulin-like growth factors on lung development in a nitrofen-induced CDH rat model. Pediatr Surg Int 27:187–192
5. Gonzalez-Reyes S, Alvarez L, Diez-Pardo JA, Tovar JA (2003) Prenatal vitamin E improves lung and heart hypoplasia in experimental diaphragmatic hernia. Pediatr Surg Int 19:331–334
6. Schmidt AF, Gonçalves FLL, Regis AC, Gallindo RM, Lourenço S (2012) Prenatal retinoic acid improves lung vascularization and VEGF expression in CDH rat. Am J Obstet Gynecol 207:76.e25–76.e32
7. Deprest J, De Coppi P (2012) Antenatal management of isolated congenital diaphragmatic hernia today and tomorrow: ongoing collaborative research and development. J Pediatr Surg 47:282–290
8. Jani J, Nicolaides KH, Keller RL, Benachi A, Peralta CF, Favre R, Moreno O, Tibboel D, Lipitz S, Eggink A, Vaast P, Allegaert K, Harrison M, Deprest J, Antenatal-CDH-Registry Group (2007) Observed to expected lung area to head circumference ratio in the prediction of survival in fetuses with isolated diaphragmatic hernia. Ultrasound Obstet Gynecol 30:67–71
9. Jani J, Valencia C, Cannie M, Vuckovic A, Sellars M, Nicolaides KH (2011) Tracheal diameter at birth in severe congenital diaphragmatic hernia treated by feto endoscopic tracheal occlusion. Prenat Diagn 31:699–704
10. de Coppi Paolo, Deprest Jan (2012) Regenerative medicine for congenital diaphragmatic hernia: regeneration for repair. Eur J Pediatr Surg 22:393–398
11. Hematti P (2008) Role of mesenchymal stromal cells in solid organ transplantation. Transpl Rev 22:262–273
12. Hoffman AM, Paxson JA, Mazan MR, Davis AM, Tyagi S, Murthy S, Ingenito EP (2011) Lung-derived mesenchymal stromal cell post-transplantation survival, persistence, paracrine expression, and repair of elastase-injured lung. Stem Cells Dev 20:1779–1792
13. Zhu X, Shi W, Tai W, Liu F (2012) The comparison of biological characteristics and multilineage differentiation of bone marrow and adipose derived mesenchymal stem cells. Cell Tissue Res 11:277–287
14. Aslam M, Baveja R, Liang OD, Fernandez-Gonzalez A, Lee C, Mitsialis SA, Kourembanas S (2009) Bone marrow stromal cells attenuate lung injury in a murine model of neonatal chronic lung disease. Am J Respir Crit Med 180:1122–1130
15. van Haaften T, Thébaud B (2006) Adult bone marrow derived stem cell for the lung: implications for pediatric lung disease. Pediatr Res 59:94–99
16. Pua JZ, Stonestreet BS, Cullen A, Shahsafaei A, Sadowska GB, Sunday ME (2005) Histochemical analyses of altered fetal lung development following single vs multiple courses of antenatal steroids. J Histochem Cytochem 53:1469–1479
17. Wu S, Platteau A, Chen S, McNamara G, Whitsett J, Bancalari E (2010) Conditional overexpression of connective tissue growth factor disrupts postnatal lung development. Am J Respir Cell Mol Biol 42:552–563
18. Kitaguchi Y, Taraseviciene-Stewart L, Hanaoka M, Natarajan R, Kraskauskas D, Voelkel N (2012) Acrolein induces endoplasmic reticulum stress and causes airspace enlargement. PLoS One 7(5):e38038. doi:10.1371/journal.pone.0038038
19. Hansmann G, Fernandez-Gonzalez A, Aslam M, Vitali SH, Martin T, Mitsialis SA, Kourembanas S (2012) Mesenchymal stem cell-mediated reversal of bronchopulmonary dysplasia and associated pulmonary hypertension. Pulm Circ 2:170–181
20. Okoye BO, Losty PD, Lloyd DA, Gosney JR (1998) Effect of prenatal glucocorticoids on pulmonary vascular muscularisation in nitrofen-induced congenital diaphragmatic hernia. J Pediatr Surg 33:76–80
21. Pozzobon M, Ghionzoli M, De Coppi P (2010) ES, iPS, MSC, and AFS cells. Stem cells exploitation for pediatric surgery: current research and perspective. Pediatr Surg Int 26:3–10
22. Crisostomo PRM, Markel TA, Wang Y, Meldrum DR (2008) Surgically relevant aspects of stem cell paracrine effects. Surgery 143:577–581
23. Ardhanareeswaran K, Miratsou M (2013) Lung stem and progenitor cells. Respiration 85:89–95
24. Keating A (2012) Mesenchymal stromal cells: new directions. Stem Cell 10:709–716
25. Ingenito EP, Tsai L, Murthy S, Tyagi S, Mazan M, Hoffman A (2012) Autologous lung-derived mesenchymal stem cell transplantation in experimental emphysema. Cell Transpl 21:175–189
26. Chen CP, Lee MY, Huang JP, Aplin JD, Wu YH, Hu CS, Chen PC, Li H, Hwang SM, Liu SH, Yang YH (2008) Trafficking of multipotent mesenchymal stromal cells from maternal circulation through the placenta involves vascular endothelial growth factor receptor-1 and integrins. Stem Cells 26:550–561
27. Badri L, Walker NM, Ohtsuka T, Wang Z, Delmar M, Flint A, Golden MP, Toews GB, Pinsky DJ, Krebsbach PH, Lama VN (2011) Epithelial interactions and local engraftment of lung-resident mesenchymal stem cells. Am J Respir Cell Mol Biol 45:809–816
28. Lee JW, Fang X, Krasnodembskaya A, Howard JP, Matthay MA (2011) Concise review: mesenchymal stem cells for acute lung injury: role of paracrine soluble factors. Stem Cells 29:913–919
29. Zhu F, Xia ZF (2013) Paracrine activity of stem cells in therapy for acute lung injury and adult respiratory distress syndrome. J Trauma Acute Care Surg 74:1351–1356
30. Conese M, Carbone A, Castellani S, Gioia SD (2013) Paracrine effects and heterogeneity of marrow-derived stem/progenitor cells: relevance for the treatment of respiratory diseases. Cell Tissues Organs 197:445–473
31. Di Bernardo J, Maiden MM, Hershenson MB, Kunisaki SM (2014) Amniotic fluid derived mesenchymal stem cells augment fetal lung growth in a nitrofen explant model. J Pediatr Surg. doi:10.1016/j.jpedsurg.2014.01.013
32. Pederiva F, Ghionzoli M, Pierro A, De Coppi P, Tovar JA (2013) Amniotic fluids stem cells rescue both in vitro and in vivo growth, innervation, and motility in nitrofen-exposed hypoplastic rat lungs through paracrine effects. Cell Transpl 22:1683–1694

Glypican 3 Expression in Pediatric Malignant Solid Tumors

Yoshiaki Kinoshita[1] Sakura Tanaka[1] Ryota Souzaki[1] Kina Miyoshi[2] Kenichi Kohashi[2] Yoshinao Oda[2] Tetsuya Nakatsura[3] Tomoaki Taguchi[1]

[1] Department of Pediatric Surgery, Kyushu University, Fukuoka, Japan
[2] Department of Anatomic Pathology, Kyushu University, Fukuoka, Japan
[3] Division of Cancer Immunotherapy, National Cancer Center Hospital East, Kashiwa, Japan

Address for correspondence Yoshiaki Kinoshita, MD, PhD, Department of Pediatric Surgery, Kyushu University, 3-1-1, Maidashi, Higashiku, Fukuoka-City, Fukuoka 812-8582, Japan (e-mail: kinoppy@pedsurg.med.kyushu-u.ac.jp).

Eur J Pediatr Surg 2015;25:138–144.

Abstract

Purpose Glypican 3 (GPC3) is one of the cell surface heparan sulfate proteoglycans that binds to the cell membrane, and it is known as an oncofetal protein in adult malignant tumors. Clinical trials using a GPC3 peptide vaccine have already been started in Japan as a new immunotherapy for hepatocellular carcinoma in adult patients. To investigate the possibility of GPC3 immunotherapy for pediatric malignant tumors, we assessed the expression of GPC3 in pediatric malignant tumors.

Methods Immunohistochemically, the GPC3 expression was examined in 159 pediatric solid tumors, including 35 cases of neuroblastoma, 30 cases of Wilms tumor, 10 cases of hepatoblastoma, 25 cases of germ cell tumors, 56 cases of rhabdomyosarcoma, and 3 cases of other tumors. In addition, to clarify the physiological expression during the fetal to neoinfantile period, autopsy specimens of subjects without any neoplastic diseases were assessed in 9 fetal cases and 21 neoinfantile cases. The serum levels of GPC3 were also analyzed using specimens obtained from 53 subjects by the sandwich enzyme-linked immunosorbent assay method.

Results Histologically, a high rate of GPC3 expression was noted in 10 (90.9%) of the 11 subjects with yolk sac tumors and 6 (60.0%) of the 10 subjects with hepatoblastoma. In addition, 9 (30.0%) of the 30 subjects with Wilms tumors and 14 (25.0%) of the 56 subjects with rhabdomyosarcoma were positive for the expression of GPC3. Concerning autopsy specimens, most of the 23 subjects younger than 7 months showed positive findings in the liver (94.7%) and kidney (81.8%). Two subjects (100%) with yolk sac tumors and six (75.0%) of the eight subjects with hepatoblastoma serologically demonstrated a high rate of positive expression. Concerning the distribution of the serum GPC3 level according to age, 8 (80.0%) of the 10 subjects younger than 1 year showed a positive finding, while only 16 (37.3%) of the 43 subjects older than 1 year showed a positive finding.

Conclusion Most cases of hepatoblastoma and yolk sac tumor, and some cases of other tumors were found to express GPC3 either histologically or serologically. On the other hand, GPC3 was physiologically expressed during the fetal and neoinfantile period under 1 year of age. Although, more preliminary data and experience are required,

Keywords
- glypican 3
- tumor marker
- immunotherapy

received
May 15, 2014
accepted after revision
July 29, 2014
published online
October 26, 2014

DOI http://dx.doi.org/10.1055/s-0034-1393961.
ISSN 0939-7248.

patients older than 1 year that show a positive finding for GPC3 are considered to be appropriate candidates to receive the new immunotherapy using GPC3 peptide vaccination.

Introduction

Glypican 3 (GPC3) is a cell surface heparan sulfate proteoglycan that is linked to the extracytoplasmic cell-surface membrane by a glycosylphosphatidylinositol anchor.[1] GPC3 is associated with cell growth, development, and the responses to various growth factors.[2] Gonzalez et al described its role as a negative regulator of inhibitory growth factors.[3] GPC3 inactivation has been found to be responsible for X-linked Simpson–Golabi–Behmel (SGB) overgrowth syndrome. In SGB syndrome, 10 to 20% of the patients described have an embryonal malignancy, including hepatoblastoma, neuroblastoma, gonadoblastoma, Wilms tumor, or hepatocellular carcinoma.[4]

Recent studies have shown that there is an overexpression of GPC3 in hepatocellular carcinoma, and has its usefulness as a novel diagnostic marker in many series.[5] Furthermore, the expression of GPC3 has also been reported in other malignant tumors, such as malignant melanoma,[8] clear cell adenocarcinoma of the ovary,[9] and malignant germ cell tumors in adult subjects.[10] Ota et al reported the immunoreactivity of adult testicular tumors, including a yolk sac tumor, teratoma, and choriocarcinoma, as well as a seminoma and embryonal carcinomas. The author demonstrated a high rate of immunoreactivity for the yolk sac tumor.[10]

GPC3 expression has not yet been widely analyzed in pediatric tumors and the roles of GPC3 expression are still unclear. The expression of GPC3 mRNA in several cell lines, including those derived from neuroblastomas, Wilms tumors, and hepatoblastomas, has been reported.[11,12] In addition, Zynger et al examined 65 cases of hepatoblastoma by immunohistochemistry and all subjects exhibited a positive reaction.[13] Zynger et al speculated that GPC3 has a role in the tumorigenesis of hepatoblastoma.

In this study, we analyzed the expression of GPC3 in pediatric malignant solid tumors and assessed the clinical implications of its expression.

Materials and Methods

The immunohistochemical studies examined 159 pediatric solid tumors, including 35 cases of neuroblastoma, 30 cases of Wilms tumor, 10 cases of hepatoblastoma, 25 cases of germ cell tumors (11 yolk sac tumors, 4 immature teratomas, and 10 mature teratomas), and 56 cases of rhabdomyosarcoma and 3 cases of other tumors (2 undifferentiated sarcomas and 1 case of Ewing sarcoma) treated at our institution. The serum levels of GCP3 were also analyzed in samples obtained from 53 subjects, including 13 cases with neuroblastoma, 10 cases of Wilms tumor, 8 cases of hepatoblastoma, 16 cases of germ cell tumors (2 cases with yolk sac tumors, 4 cases with immature teratomas, and 10 cases with mature teratomas), 3 cases of rhabdomyosarcoma, and 3 cases of other tumors by the sandwich enzyme-linked immunosorbent assay (ELISA) method using a GPC3 ELISA kit (Bio Mosaics, Burlington, Vermont, United States).

In addition, to clarify the physiological expression during the fetal to neoinfantile period, autopsy specimens from subjects without any neoplastic disease were assessed by immunohistochemistry. These included samples from 9 fetal cases (age, 19–41 weeks) and 21 neoinfantile cases.

For the immunohistochemical analysis the streptavidin-biotin-peroxidase method (Histofine SAB-PO Kit, Nichirei, Tokyo, Japan) was used. A GPC3 monoclonal antibody (Bio Mosaics) was used at 1:200 dilution.

The serum levels of GPC3 were analyzed by a sandwich ELISA method using an ELISA kit. The samples were diluted at 1:4 and 100 µL of samples or of GPC3 standards were pipetted into the appropriate wells. Covered wells were incubated overnight at 2 to 8°C. After washing the wells five times with wash buffer, 200 µL of a biotin-conjugated anti-GPC3 antibody was pipetted into each well. After overnight incubation, the wells were washed with buffer and 200 µL of streptavidin-horseradish peroxidase conjugated diluents were added to each well. After 30 minutes of incubation, 200 µL of tetramethylbenzidine substrate solution was added to each well for 30 minutes. After these procedures, the absorbance of each well was analyzed by a spectrophotometric plate reader. Based on the data of healthy adult subjects with the standard deviation, the cut-off level for GPC3 was defined as 178 ng/mL in this study.

The patient's parents provided consent for obtaining tumor and tissue preservation and for the subsequent biological analyses. This study was performed according to the Ethical Guidelines for Clinical Research published by the Ministry of Health, Labor, and Welfare of Japan on July 30, 2003.

Results

Histologically, a high rate of GPC3 expression was noted in 10 (90.9%) of the 11 subjects with yolk sac tumors and in 6 (60.0%) of the 10 subjects with hepatoblastoma (►Table 1 and ►Figs. 1a, b). In addition, 9 (30.0%) of the 30 subjects with Wilms tumor (►Fig. 1c), 14 (25.0%) of the 56 subjects with rhabdomyosarcoma, and 1 (2.9%) of the 35 subjects with neuroblastoma were positive for the expression of GPC3.

Similarly, 2 subjects (100%) with yolk sac tumors and 6 (75.0%) of the 8 subjects with hepatoblastoma serologically demonstrated a high rate of positive expression, while 1 (33.3%) of the 3 subjects with rhabdomyosarcoma, 4 (30.7%) of the 13 subjects with neuroblastoma, and 1

Table 1 The results of the immunohistochemical and serological analysis of glypican 3

Histology		GPC3	
		Tissue GPC3 (immunohistochemistry)	Serum GPC3 (ELISA)
HB	Hepatoblastoma	6/10 (60.0%)	6/8 (75.0%)
NBs	Neuroblastoma	1/35 (2.9%)	4/13 (27.3%)
WT	Wilms tumor	9/30 (30.0%)	1/10 (10.0%)
RMS	Rhabdomyosarcoma	14/56 (25.0%)	1/3 (33.3%)
GCT	Yolk sac tumor	10/11 (90.9%)	2/2 (100%)
	Immature teratoma	1/4 (25.0%)	3/4 (75.0%)
	Mature teratoma	0/10 (0.0%)	5/10 (50.0%)
Others	Undifferentiated sarcoma	1/2 (50%)	2/2 (100%)
	Ewing sarcoma	0/1 (0.0%)	0/1 (0.0%)
Total number		159	53

Abbreviations: ELISA, enzyme-linked immunosorbent assay; GCT, germ cell tumor; GPC3, glypican 3; HB, hepatoblastoma; NBs, neuroblastoma and associated tumor; RMS, rhabdomyosarcoma; WT, Wilms tumor.

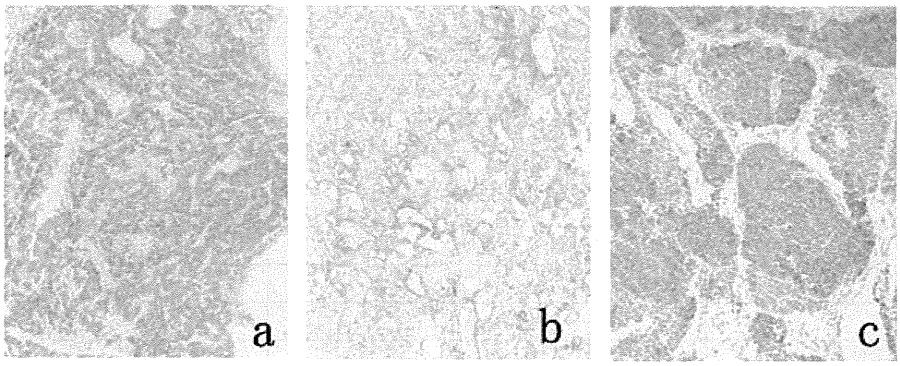

Fig. 1 Immunohistochemical findings: (a) hepatoblastoma, 2-year old; (b) yolk sac tumor, 12-year old; (c) Wilms tumor, 3-year old.

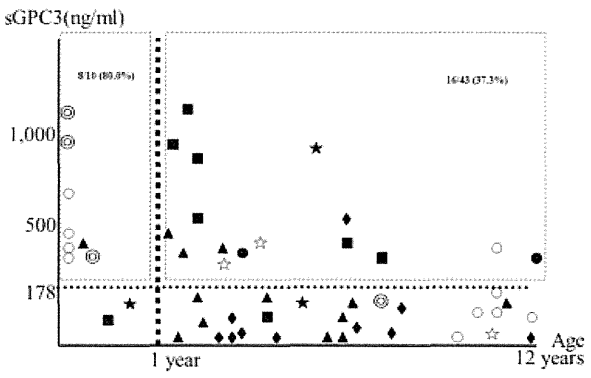

Fig. 2 The distribution of the serum glypican 3 (GPC3) levels according to age. Samples from 8/10 (80.0%) patients younger than 1 year were serologically GPC3-positive, while only samples from 16/43 (37.2%) patients older than 1 year were serologically GPC3-positive. ■, hepatoblastoma; ▲, neuroblastoma and associated tumors; ♦, Wilms tumor; germ cell tumor; ●, yolk sac tumor; ◎, immature teratoma; ○, mature teratoma; ★, rhabdomyosarcoma; ☆, others.

(10.0%) of the 10 subjects with Wilms tumor demonstrated a positive finding (►Fig. 2).

Concerning the distribution of the serum GPC3 level according to age, 8 (80.0%) of the 10 subjects younger than 1 year showed a positive finding. In contrast, only 16 (37.2%) of the 43 subjects older than 1 year showed a positive finding.

Concerning the autopsy specimens, most of the 23 subjects younger than 7 months (including 9 fetal and 14 neoinfantile subjects) showed positive findings in the liver (94.7%) and kidney (81.8%) (►Table 2) (►Figs. 3a–d). The other six subjects older than 1 year did not demonstrate a positive finding in any organ.

The clinical course of one representative case was as follows (►Fig. 4). The subject had an undifferentiated sarcoma that was diagnosed when the patient was 4 years and 6 months old. The serum α-fetoprotein (AFP) level was low, the serum GPC3 level was 334 ng/mL, and the biopsy specimen was immunohistochemically positive for GPC3. The level of serum GPC3 normalized following preoperative intensive

Table 2 The results of the immunohistochemical analysis for autopsy specimens

Age	CNS	Heart	Lung	Liver	Kidney	Pancreas	Spleen	Adrenal gland	Thymus	GI tract
19 wk	–	ND	–	+	+	+	–	ND	ND	–
19 wk	–	ND	–	ND	+	ND	–	ND	–	ND
21 wk	ND	–	–	+	+	–	–	–	ND	ND
21 wk	–	–	–	+	+	–	–	ND	–	–
24 wk	–	–	–	+	+	ND	–	ND	ND	–
24 wk	–	–	–	+	+	ND	–	ND	ND	–
32 wk	–	–	–	+	+	–	–	–	–	–
38 wk	–	–	–	+	+	ND	–	–	+	–
41 wk	–	–	–	+	ND	ND	–	–	–	ND
0 d	–	–	–	+	+	+	–	–	–	–
0 d	ND	–	–	+	+	–	–	–	–	–
0 d	–	–	–	ND	+	ND	–	ND	ND	–
0 d	–	–	–	ND	–	ND	–	ND	ND	–
0 d	ND	–	–	+	+	–	–	–	ND	–
1 d	ND	–	–	+	+	ND	–	–	–	ND
12 d	ND	–	ND	+	–	–	–	–	–	–
14 d	–	–	–	ND	+	+	–	–	–	–
1 mo	ND	–	–	+	–	–	–	–	–	–
3 mo	ND	–	–	+	–	–	–	ND	–	ND
4 mo	ND	–	–	+	+	–	–	ND	–	ND
6 mo	ND	–	–	+	+	–	–	–	ND	–
6 mo	ND	ND	–	–	+	–	–	–	ND	–
7 mo	ND	–	–	+	+	–	–	ND	–	ND
8 mo	ND	–	–	ND	ND	ND	ND	ND	ND	ND
1 y 0 mo	–	–	–	ND	–	–	ND	–	–	ND
1 y 0 mo	–	–	–	–	–	–	–	–	ND	–
1 y 4 mo	–	–	–	ND	–	–	–	–	ND	–
9 y	–	ND	ND	ND	ND	ND	ND	ND	ND	ND
9 y	ND	–	–	ND	ND	ND	ND	ND	–	ND
10 y	–	–	–	–	–	–	–	–	ND	–

Abbreviations: CNS, central nervous system; +, positive; –, negative; ND, not done.

chemotherapy and was maintained within a normal range thereafter. Furthermore, the specimen obtained by radical surgery showed no viable tumor cells and the tissue was immunohistochemically negative for GPC3. After the treatment, the patient has survived for 5 years without any events and the patient's GPC3 level is normal. In this case, the serum GPC3 level was useful as an independent tumor marker.

Discussion

In recent years, several authors have reported the diagnostic value of the serum GPC3 level in hepatocellular carcinomas and other kinds of malignant tumors in adults. In the field of GPC3 research, the expression levels in fetal tissue have been discussed by several authors. Immunohistochemically, three cases of fetal liver tissue were found to be positive, although the benign pediatric liver was negative.[13] In this way, GPC3 has been considered to be a kind of oncofetal protein and to be associated with tumorigenesis in pediatric malignant tumors. However, the clinical implications of the GPC3 expression levels as a diagnostic marker or for the monitoring of tumor progression or curability have not yet been sufficiently analyzed.

From the current data, most hepatoblastomas and yolk sac tumors showed positive findings for both serum and tissue GPC3. In most subjects younger than 1 year, there was a tendency toward a higher level of GPC3 expression compared with subjects older than 1 year. In particular, newborn patients with germ cell tumors, including mature and immature teratomas, exhibited a high level of serum GPC3. Based

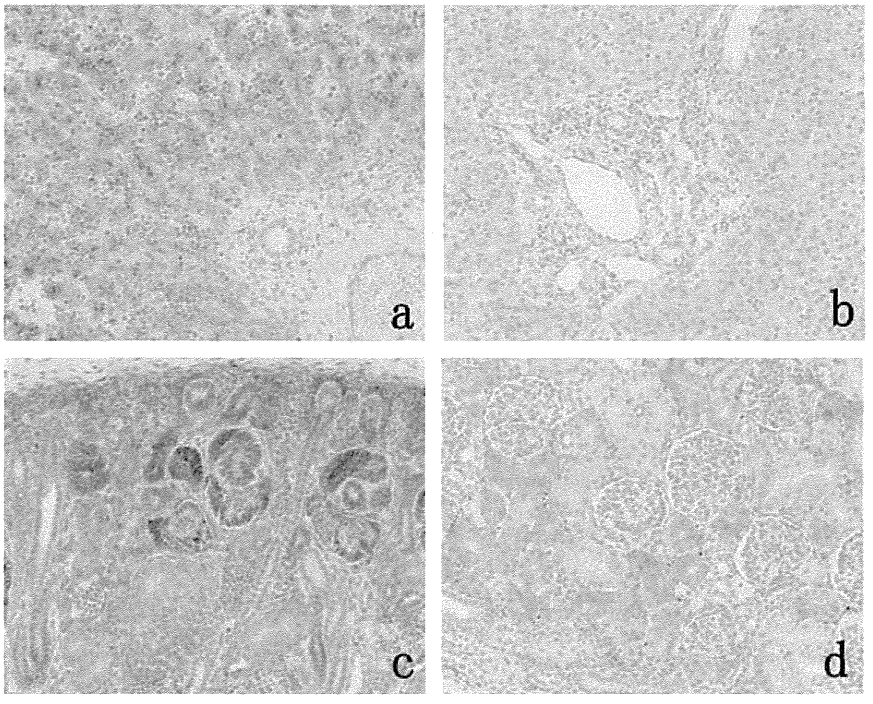

Fig. 3 Immunohistochemical findings for autopsy specimens: (a) fetal liver, 19 weeks, strongly positive; (b) infantile liver, 7 months, moderately positive; (c) fetal kidney, 19 weeks, strongly positive; (d) infantile kidney, 7 months, moderately positive.

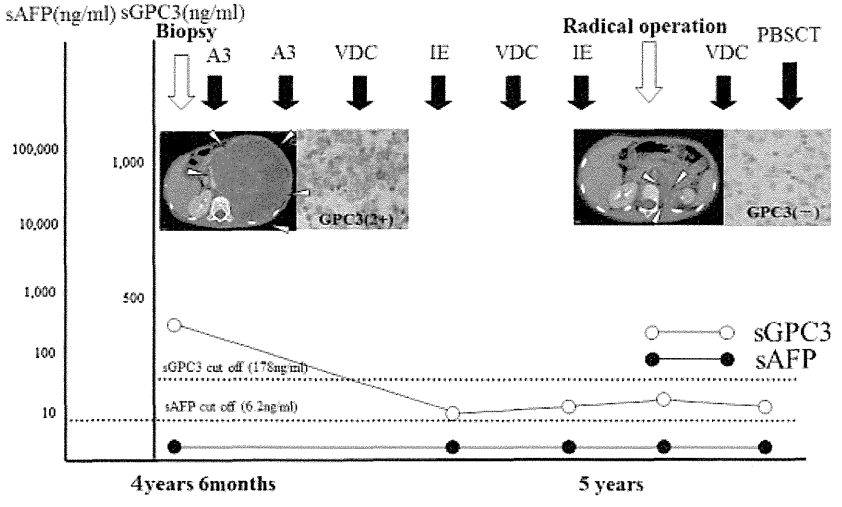

Fig. 4 Clinical course of one case with undifferentiated sarcoma. A3, vincristine + THP-adriamycin + cyclophosphamide + cisplatin; IE, ifosfamide + etoposide; sAFP, serum α-fetoprotein; sGPC3, serum glypican 3; VDC, vincristine + doxorubicin + cyclophosphamide.

on the results of autopsy specimens, we can speculate that GPC3 expression can be observed from the fetal to early neoinfantile period for younger than 1 year regardless of whether malignancy is present. For the subjects older than 1 year, the data from patients who were positive for serum GPC3 but negative for serum AFP imply that GPC3 may be an independent novel tumor marker.

The role of GPC3 as a novel tumor marker for hepatocellular carcinoma in adults has been widely debated in recent studies. A trial using GPC3-targeted immunotherapy for the prevention of cancer development and recurrence has already begun.[14] The same trial protocol would be acceptable to treat and prevent pediatric malignant tumors. However, the number of this series is small, more preliminary data and experience are required to conclude this suitability for immunotherapy.

Conclusion

Most cases of hepatoblastoma, yolk sac tumors and some cases of neuroblastoma, Wilms tumor, and rhabdomyosarcoma were found to express GPC3 either histologically or serologically. On the other hand, GPC3 was also physiologically expressed during the fetal and neoinfantile period in

subjects younger than 1 year. Because the patients older than 1 year who show a positive finding for GPC3 are considered to be appropriate candidates to receive the new immunotherapy using the GPC3 peptide vaccination.

Conflict of Interest
None.

References

1 Filmus J. Glypicans in growth control and cancer. Glycobiology 2001;11(3):19R–23R
2 Song HH, Filmus J. The role of glypicans in mammalian development. Biochim Biophys Acta 2002;1573(3):241–246
3 Gonzalez AD, Kaya M, Shi W, et al. OCI-5/GPC3, a glypican encoded by a gene that is mutated in the Simpson-Golabi-Behmel overgrowth syndrome, induces apoptosis in a cell line-specific manner. J Cell Biol 1998;141(6):1407–1414
4 Lapunzina P. Risk of tumorigenesis in overgrowth syndromes: a comprehensive review. Am J Med Genet C Semin Med Genet 2005; 137C(1):53–71
5 Hippo Y, Watanabe K, Watanabe A, et al. Identification of soluble NH2-terminal fragment of glypican-3 as a serological marker for early-stage hepatocellular carcinoma. Cancer Res 2004;64(7): 2418–2423
6 Capurro M, Wanless IR, Sherman M, et al. Glypican-3: a novel serum and histochemical marker for hepatocellular carcinoma. Gastroenterology 2003;125(1):89–97
7 Nakatsura T, Yoshitake Y, Senju S, et al. Glypican-3, overexpressed specifically in human hepatocellular carcinoma, is a novel tumor marker. Biochem Biophys Res Commun 2003;306(1):16–25
8 Nakatsura T, Kageshita T, Ito S, et al. Identification of glypican-3 as a novel tumor marker for melanoma. Clin Cancer Res 2004;10(19): 6612–6621
9 Maeda D, Ota S, Takazawa Y, et al. Glypican-3 expression in clear cell adenocarcinoma of the ovary. Mod Pathol 2009;22(6): 824–832
10 Ota S, Hishinuma M, Yamauchi N, et al. Oncofetal protein glypican-3 in testicular germ-cell tumor. Virchows Arch 2006;449(3): 308–314
11 Saikali Z, Sinnett D. Expression of glypican 3 (GPC3) in embryonal tumors. Int J Cancer 2000;89(5):418–422
12 Toretsky JA, Zitomersky NL, Eskenazi AE, et al. Glypican-3 expression in Wilms tumor and hepatoblastoma. J Pediatr Hematol Oncol 2001;23(8):496–499
13 Zynger DL, Gupta A, Luan C, Chou PM, Yang GY, Yang XJ. Expression of glypican 3 in hepatoblastoma: an immunohistochemical study of 65 cases. Hum Pathol 2008;39(2):224–230
14 Nishimura Y, Nakatsura T, Senju S. Usefulness of a novel oncofetal antigen, glypican-3, for diagnosis and immunotherapy of hepatocellular carcinoma [in Japanese]. Nihon Rinsho Meneki Gakkai Kaishi 2008;31(5):383–391